



Evaluation of kinetic moduli and soil competence scale of soil profiles in Jizan area, southwestern Saudi Arabia

Kamal Abdelrahman^{1,2} · Elkhedr Ibrahim¹ · Saleh Qaysi¹ · Saad Mogren¹ · Faisal Zaidi¹ · Habes Ghrefat¹

Received: 22 August 2020 / Accepted: 16 December 2020 / Published online: 26 January 2021
© Saudi Society for Geosciences 2021

Abstract

The P-wave seismic refraction, multi-channel analysis of surface waves, and standard penetration test data were integrated in this study to assess the heterogeneity of the soil profiles of Jizan area with emphasis on dynamic moduli and the soil competence scale. The standard penetration test data were acquired from 120 boreholes in Jizan City and analyzed to construct a soil profile till 20 m depth. Moreover, fourteen profiles of seismic refraction and multichannel analysis of surface waves were created near boreholes to estimate 1D and 2D velocity models for P- and S-wave velocities. The depth of the soil profiles has been identified where it ranges from 0 down to 31.5 m. Based on results, Young's modulus, bulk modulus, rigidity modulus, Poisson's ratio, and ultimate bearing capacity vary in the ranges of $0.3\text{--}3.2 \times 10^9$, $0.2\text{--}3.3 \times 10^9$, $0.12\text{--}1.35 \times 10^9$, 0.21–0.34, and $0.04\text{--}1.05 \text{ kg/cm}^2$, respectively, while the mean values of the N value, density gradient, concentration index, material index, and stress ratio range from 2 to 30, from 1.13 to 1.51, from 4.0 to 5.8, from -0.34 to $+0.16$, and from 0.27 to 0.51, respectively, through the area. Lithological heterogeneities and dynamic and geotechnical parameters were quantified for the two upper layers. The topmost layer has varying features down to a depth of about 8 m, indicating a loose to moderately dense soil overlying the second layer with medium to dense deposits. The changing of soil profiles either laterally and vertically, and their corresponding dynamic and geotechnical properties, either generate new or increase the pre-existing geotechnical and engineering problems. Engineering treatments of very soft (liquefiable) soils are highly recommended before constructing new buildings and infrastructure in Jizan City.

Keywords Standard penetration test · Multichannel analysis of surface waves · Dynamic and geotechnical properties · Jizan City · Saudi Arabia

Introduction

Nowadays, it has been noticed that the heterogeneities of the topsoil profile play an effective role in the widespread severe damage and foundation failure in coastal areas. Ground conditions become one of the devastating types of natural disasters that the world is currently facing. The

scale of development in cities where ground conditions change significantly adds to the impacts of damage. Burland (2007) stated that establishing the soil profile is the critical factor of site investigation. Moreover, it was indicated that the occurrence of sabkha soil with significant thickness hasten the structural damages.

In recent years, several authors have studied the problems related to ground conditions. Stipho (1984) clarified the relationship between soil profiles and foundation problems in the desert region of the Middle East. Abu-Hajar (1991) inspected the ground setting in Jeddah City and foundation design. Dhowian and Erol (1993) investigated ground conditions and associated structural problems in the Jizan and Tabuk regions. Matsah and Hossain (1993) studied the ground conditions in Al-Madinah Al-Munawarah, Saudi Arabia. Anbazhagan and Sitharam (2006) assessed dynamic characteristics for ground outlines using the multichannel analysis of surface

This article is part of the Topical Collection on *Advances of Geophysical and Geological Prospection for Natural Resources in Egypt and the Middle East*

✉ Kamal Abdelrahman
khassanein@ksu.edu.sa

¹ Department of Geology and Geophysics, College of Science, King Saud University, Riyadh, Saudi Arabia

² Seismology Department, National Research Institute of Astronomy and Geophysics, Cairo, Egypt

waves (MASW) technique for Bangalore City. Shaaban et al. (2013) tested ground subsidence variations near the City Star Shopping Mall in Cairo, where a great building was tilted. Roy and Bhalla (2017) examined the role of soil geotechnical properties in civil engineering structures. Ravi (2017) conducted an intensive geotechnical survey under severe ground conditions in India. Abdelrahman et al. (2020) evaluated the ground conditions in Makkah al-Mukarramah City, Saudi Arabia. Alhumimidi (2020) studied the hazardous impacts of shallow deposits through Jizan City in terms of thickness and some geotechnical parameters.

Today, seismic investigations are of utmost importance for calculating the dynamic properties of soil (Imai 1975; Stumpel et al. 1984; Sjogren et al. 1979; Abd El Rahman and Abd El Latif 1990; Abd El Rahman et al. 1991). Jizan City is located in southwestern Saudi Arabia along the Red Sea coast (Fig. 1). Due to heterogeneities in thicknesses and lithofacies, with significant variations over short distances, the city suffers from geotechnical problems. This study aims to delineate the geological conditions of Jizan City and evaluate the dynamic and geotechnical properties of the entire city.

Geological setting and geotechnical problems

The coastal plain of the Jizan region is entirely flat, except for the Jizan Salt Dome, which rises 50 m above sea level as indicated by Erol and Dhowian (1988) (Fig. 2). The drilled borehole indicates the local lithological variation (Hodgson et al. 1989, Dhowian et al. 1987; Al-hadad et al. 2001; Al-Farraj 2008; Mahfouz 2016) through the city where three units of sabkha are revealed (Table 1). The geotechnical problems in the city are clarified by Hodgson et al. (1989); Al-Amoudi (1992), Al-Amoudi et al. (1992), Amin (2004), and Arifuzzaman et al. (2016). Subsidence is the major aspect which caused

extreme damage due to the generation of cavities from the dissolution of subsurface salt rock (Fig. 3). Ghazali et al. (1986) clarified the deterioration of soils as they accumulate moisture, whether due to domestic drainage from leaking water supply systems and septic tanks and/or regular heavy rain drainage. Arifuzzaman et al. (2016) summarized Sabkha's potential problems as a rapid decline in soil strength due to water supplementation or flooding, and changes in soil compressibility characteristics within a specific area that could lead to substantial differential settlements. Gypsum ($\text{CaSO}_4 \cdot 2\text{H}_2\text{O}$) includes excessive hydration in hot and arid conditions thereby forming anhydrite (CaSO_4).

Methodology

The standard penetration test (SPT) is the most common test for classifying the type of soil where SPT values correlated well with soil density (Terzaghi 1940; Terzaghi and Peck 1948). There are several correlations between the number of SPT and different soil properties, including density of sand, unconfined compressive strength of clay, and allowable bearing pressure of sand and clay (Kulhawy and Mayne 1990; Bowles 1997; Aggour and Radding 2001; Liu et al., 2015).

For estimating P- and S-wave velocities, refraction seismic and MASW are commonly applicable methods. MASW directly evaluates the shear wave velocity (V_S) which is an important parameter for soil profiles and geotechnical characteristics (Kramer 1996; Miller et al. 1999; Park et al. 1999; Xia et al. 1999; Anderson et al. 2003). Based on these velocities, the dynamic and geotechnical constants such as density (ρ), stress ratio (S_i), Poisson's ratio (ν), rigidity modulus (μ), Young's modulus (E), and bulk modulus (B) have been calculated using the equations in Tables 1 and 2.

Table 1 The relationships of dynamic parameters used

Parameters	Used equations	References
Poisson's ratio	$\sigma = \frac{1}{2} \left(1 - \left\{ \frac{1}{\left(\left(\frac{V_P}{V_S} \right)^2 - 1\right)} \right\} \right)$	Adams (1951)
Young's modulus	$E = \rho \left[\frac{(3V_P^2 - 4V_S^2)}{\left(\left(\frac{V_P}{V_S} \right)^2 - 1\right)} \right]$	Adams (1951)
Bulk modulus	$k = \frac{E}{3(1-2\sigma)}$	
Shear modulus	$\mu = \frac{E}{2(1+\sigma)}$	

Where V_P and V_S are P- and S-wave velocities respectively

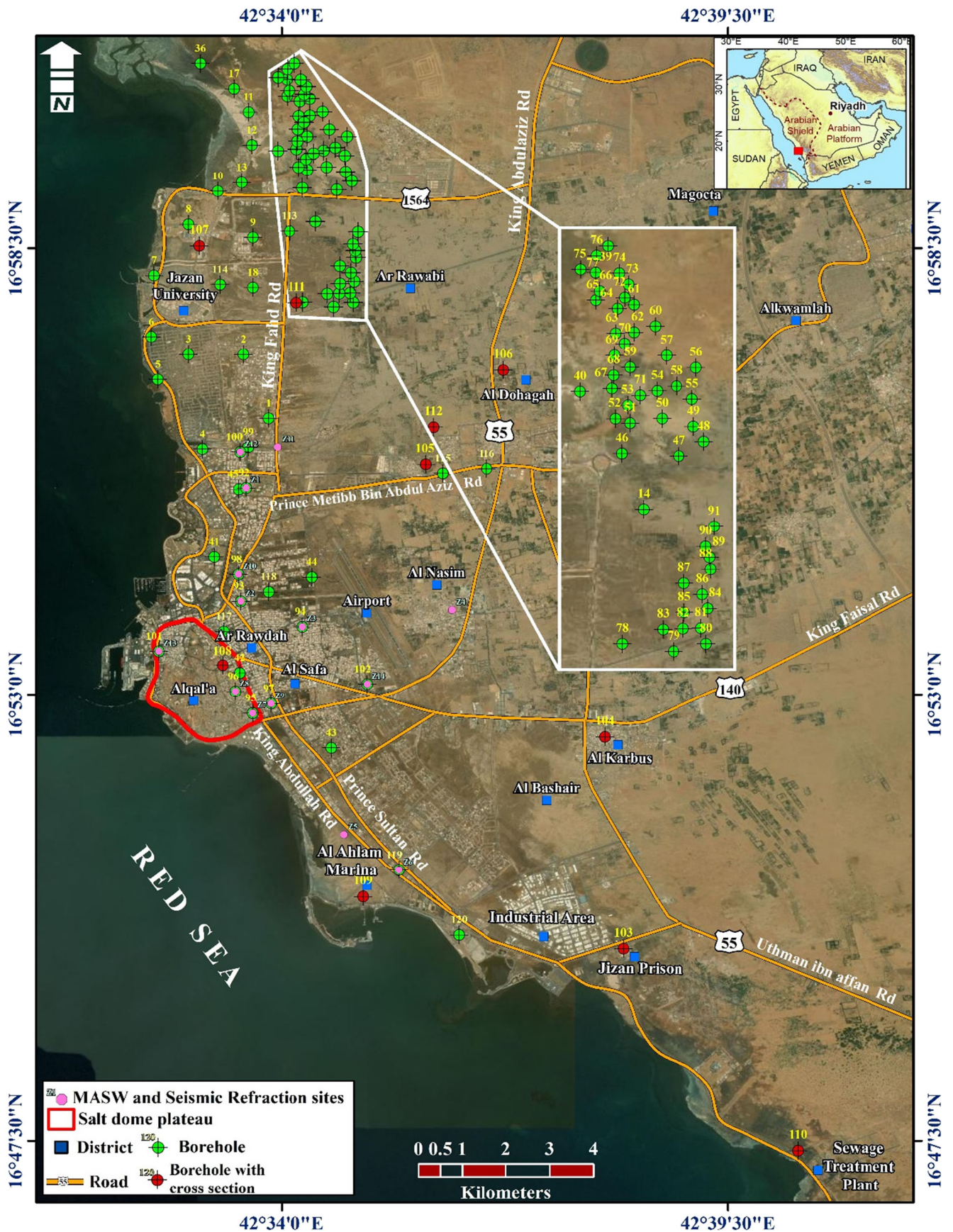


Fig. 1 Location map of the Jizan studied area

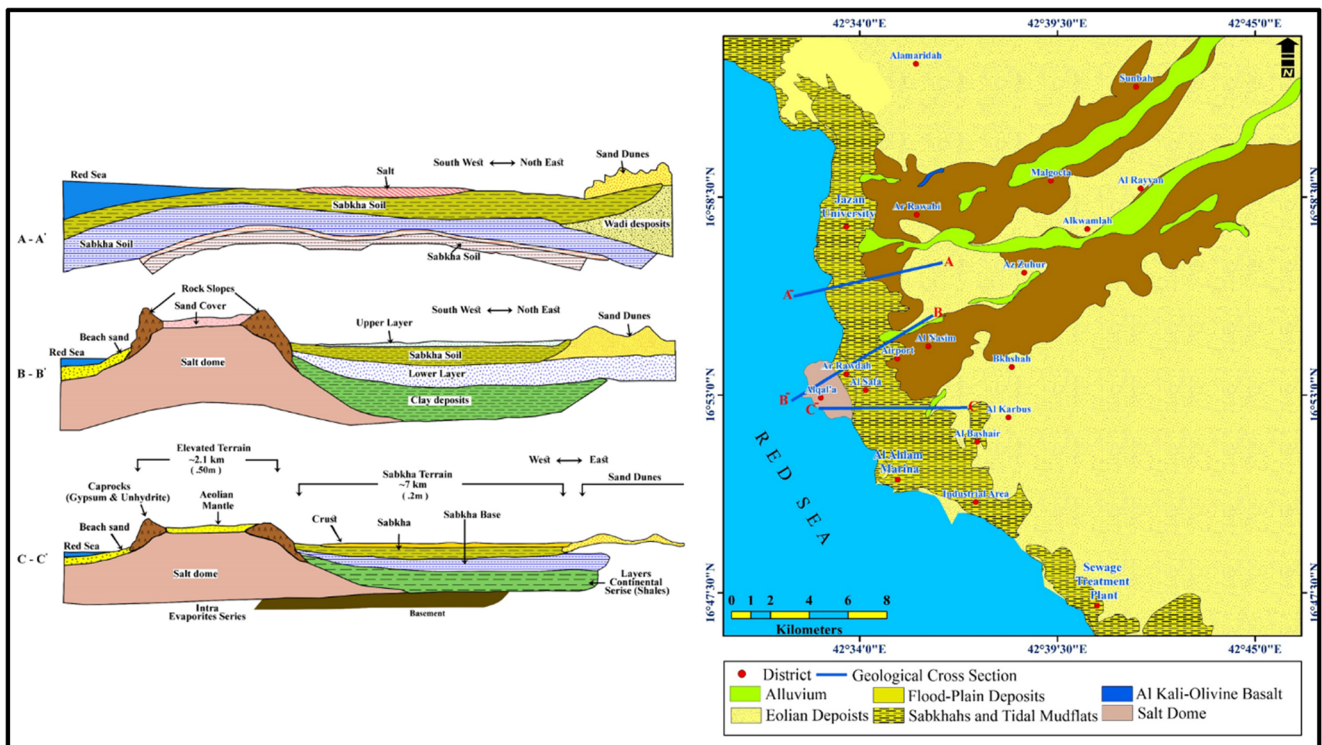


Fig. 2 Geologic map of the investigated area (modified after Blank et al. 1986)

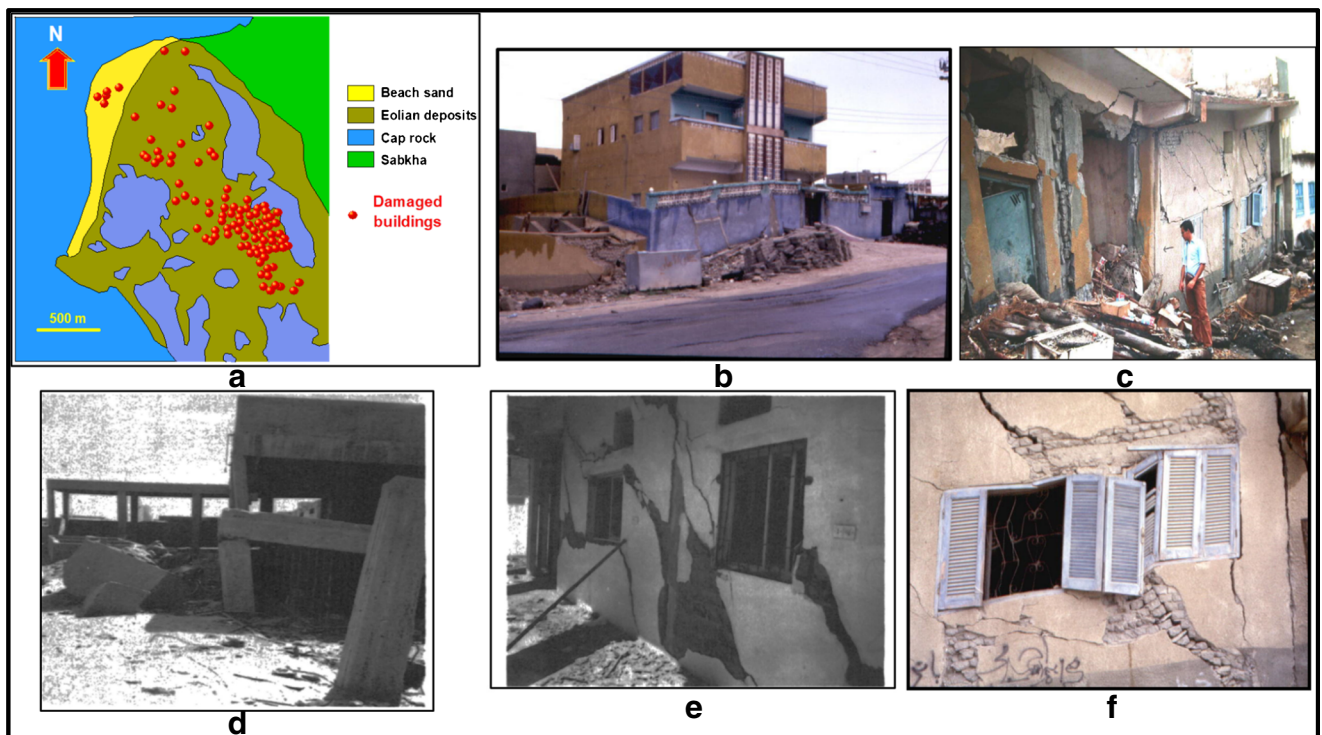


Fig. 3 Geotechnical problems and ground failure of the Jizan area; a geology of old Jizan and the locations of damaged buildings while images from b to f are examples of damaged buildings

Table 2 Geotechnical parameters and the used equations

Parameter	Used equation	Reference
Concentration index	$C_i = \frac{\left[3-4 \left(\frac{v^2}{V_p^2} \right) \right]}{\left[1-2 \left(\frac{v^2}{V_p^2} \right) \right]}$	Abd El-Rahman (1991)
Material index	$v = \frac{(\mu+\lambda)}{(\mu+\lambda)} = (1-4\sigma)$	Abd El-Rahman (1989)
Stress Ratio	$S_i = \left[1-2 \left(\frac{V^2}{V_p^2} \right) \right] = (C_i-2)^{-1}$	Abd El-Rahman (1991)

Data acquisition

The data acquired in this study includes two main data categories: (1) The fundamental information gathered was SPT-*N* values, grain size, and soil classification. Soil profiles were collected from 120 boreholes distributed throughout the Jizan area (Fig. 1). The maximum depths of these boreholes were in the following ranges: 25 m on the Jizan University campus, 8–10 m in old Jizan City and central Alkarboos Village, 16 m in Jizan Prison, and 20 m in the sewage treatment plant (in

southern Jizan), and (2) MASW and seismic refraction surveying profiles at selected sites near the drilled geotechnical boreholes throughout the city. In this study, the MASW technique was performed along 14 profiles (Fig. 1) using a 24-channel array of vertical broadband geophones (4.5 Hz) with 1 m spacing and accelerated weight drop as seismic energy source. As a source, three vertically stacked impacts of hydraulic weight drop were used on a square plate. Seismodule Controller Software (SCS) of Geometrics Inc., USA, was used for data acquisition.

Table 3 Geotechnical properties of the ground profile in borehole nos. 102, 103, 108, and 109

Average thickness (m)	Lithology	SPT
Borehole no. 102		
0.0–4.8	Silty sand (very loose to medium dense, gray, dry to wet)	9–16
4.8–9.6	Clayey silt (medium stiff to stiff, dark gray, wet)	1–6
> 9.6	Silty sand (medium dense to very dense, brown, wet)	Variable up to refusal
Borehole no. 103		
0.0–4.5	Sand (calcareous, fine to medium, traces of silt), light gray	11–27
4.5–6.0	Sand (calcareous, fine, some silt traces of peat), gray	16
6.0–9.5	Sand (fine to medium, some silt and calcareous matter), light brown	17–21
9.5–12.0	Sand (fine, silty, traces of peat), gray	23–32
12.0–15.0	Sand (medium to fine, some silt and calcareous matter), light brown	25–33
Borehole no. 108		
0.0–2.0	Silty sand with gravel, very dense, gray, dry	23–25
2.0–4.0	Silty sand, medium dense to dense, light gray, wet	1–5
4.0–11.0	Clayey silt, medium stiff to very stiff, dark gray, wet	10–26
> 11.0	Silty sand, medium dense to very dense, dark gray to gray, wet	26–45
Borehole no. 109		
0.0–1.5	Silty sand (fine to medium, traces of calcareous matters), mica, brown	2–4
1.5–3.0	Sand and clayey silt, calc., fine to medium sand grains, loose, traces of broken shells and mica, brown	3–7
3.0–4.5	Sand with broken shells, calc., medium to fine sand grains, loose, with broken shells, some silt traces, light gray	5–12
4.5–7.5	Broken shells and sand, calc., medium to fine sand grains, medium dense, with broken shells, some silt and light gray	3–11
7.5–10.0	Silty sand, calc., poorly graded medium to fine sand grains, medium dense, some broken shells, traces of organic matter (peat) & mica, dark gray	12–17

Table 4 Soil description with respect to Poisson’s ratio and material index (after Birch 1966, Tatham 1982)

Soil parameter	Incompetent to slightly competent materials	Fairly to moderately competent materials	Competent materials	Very highly competent materials
Poisson’s ratio (σ)	0.41 to 0.49	0.35 to 0.27	0.25 to 0.16	0.12 to 0.03
Material index (ν)	- 0.5 to - 1	- 0.5 to 0.0	0.0 to 0.5	> 0.5

Fourteen profiles of seismic refraction were studied along MASW profiles to construct an initial model for shear wave velocity modeling. These data were collected using 24 channels of a Geometrics StrataVisor-NZ seismograph with 5 m geophone spacing. The data files contained the precise position and shot point for each geophone, as measured by the field-synchronized GPS instrument. Furthermore, five shooting points were used along with the profile. For the generation of the P-wave, a metallic striker plate was vertically impacted using a hydraulic weight drop as the seismic energy source. The number of stacks varied between 5 and 40 at some shot points along with the profile.

Data analysis and results

Soil profiles have been collected from 120 boreholes distributed all over Jizan City and were analyzed in terms of depth and lithology where the depth of soil profiles varied considerably (Table 3). These profiles displayed several layers with

different lithologies. Four soil sections were constructed connecting ten boreholes in the area (Fig. 4). Figure 4 shows seven types of soil as follows:

1. Fill material: brown sand, fine to medium-fine gravel, traces of silt with calcareous material at Jizan University. Very dense, gray, dry, silty sand with gravel in the center of Jizan City
2. Sand: light gray, gray to light brown, fine to medium, traces of silt, broken shells with calcareous material
3. Broken shells: gray, fine to medium-size sand, medium to fine silt, and calcareous material
4. Broken shells and sand: light-gray calcareous, medium to fine sand, moderately dense, broken shells, some silt, and traces of mica
5. Silty sand: This soil varied considerably throughout the area. Light gray to yellowish brown, wet, moderately dense to dense in the central zone of Jizan City. Brown, fine to medium sand, traces of calcareous material with mica at Al Ahlam Marina to the south of Jizan City

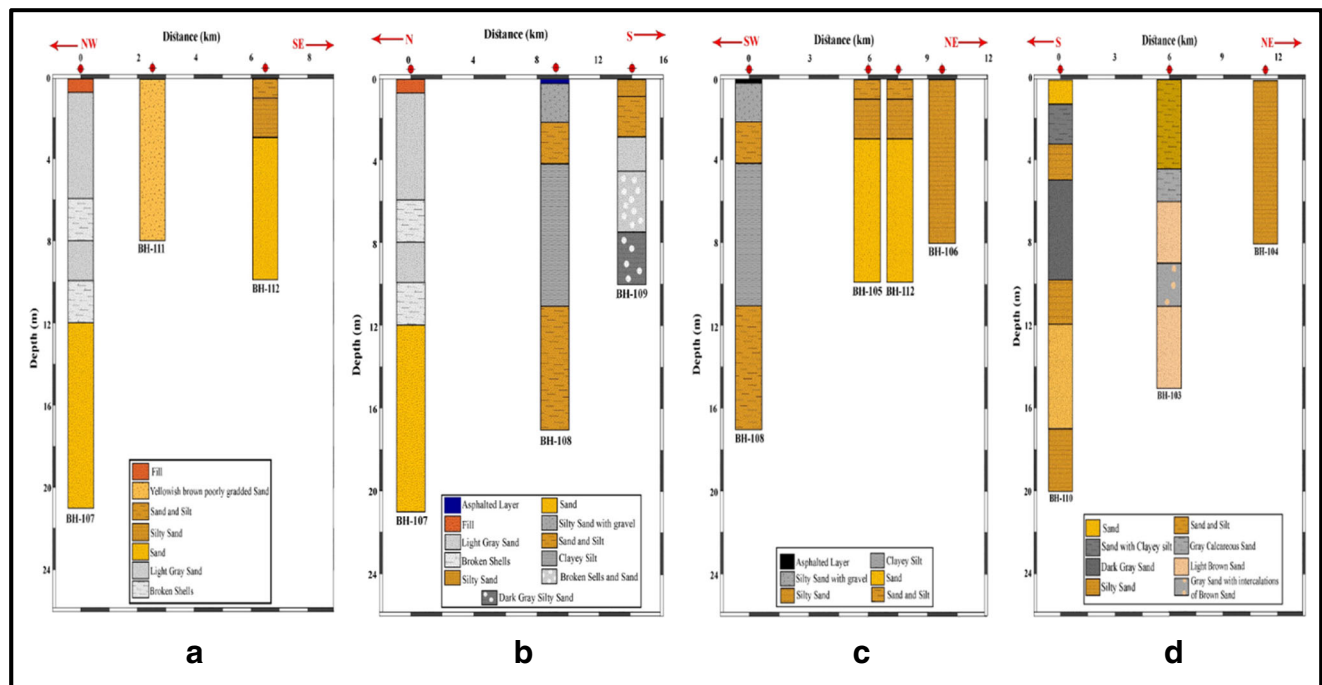


Fig. 4 Soil profiles collected from different sites through the Jizan area

Table 5 Ranges of the concentration index and stress ratio correspondent to soil competent degree (after Abd El Rahman 1989)

	Weak (Incompetent)		Fair (Fairly competent)		Good (Competent)
	Very soft	Soft	Fairly compacted	Moderately compacted	Compacted
Concentration index (C_i)	3.5–4.0	4.0–4.5	4.5–5.0	5.0–5.5	5.5–6.0
Stress ratio (S_i)	0.70–0.61	0.61–0.52	0.52–0.43	0.43–0.34	0.34–0.25

- 6. Clayey silt: dark gray, wet, moderately to extremely stiff
- 7. Sand with clayey silt: brown to blackish, calcareous, fine to medium sand, loose with traces of broken shells and mica
- 8. Clayey silty sand (organic, peat): poorly graded, fine to medium, with organic matter

Seismic refraction data was processed using *SeisImager/ 2D* software based on the nonlinear travel-time method. The recorded waveforms were filtered to remove high-frequency noise. The first break in each waveform was selected using *Pickwin* software. The layer allocation depth model was built using *Plotrefa* software for all measurement sites. Next, time inversion, linear least squares combination, and delay time analysis were used to invert the first-arrival into a 2D velocity model (Fig. 5). MASW data was processed using *RadExPro software*, a seismic processing software system created by DECO Geophysical Software Company. The MASW data was subjected to a series of processing steps to obtain 1D and 2D velocity models by inverting the corresponding dispersion curves. Figure 6 shows the 1D velocity model for 14 MASW sites.

Dynamic and geotechnical property assessment

The dynamic and geotechnical parameters were determined using the relationships shown in Tables 2 and 3, respectively. The results were then compared to the standards shown in Tables 4, 5, and 6. It is worth mentioning that changes in velocity with depth reflect changes in dynamic and geotechnical properties or layer types.

Dynamic moduli

The weaker materials have higher Poisson’s ratios and vice versa. The Poisson’s ratio of fluids is 0.5, but it approaches zero for very hard rocks. A negative Poisson’s ratio is recorded for very hard, indurated, and anisotropic rocks. The Poisson’s ratio (σ) in the study area varied between 0.246 and 0.253 (Fig. 7) for the soil profiles, indicating less competent materials. Young’s modulus (E) represents the elastic stiffness of a material and is one of the essential parameters in foundation design. In the Jizan study area, E values ranged from 2.94 to 70.92×10^8 dyn/cm² (Fig. 8). Shear modulus (G)

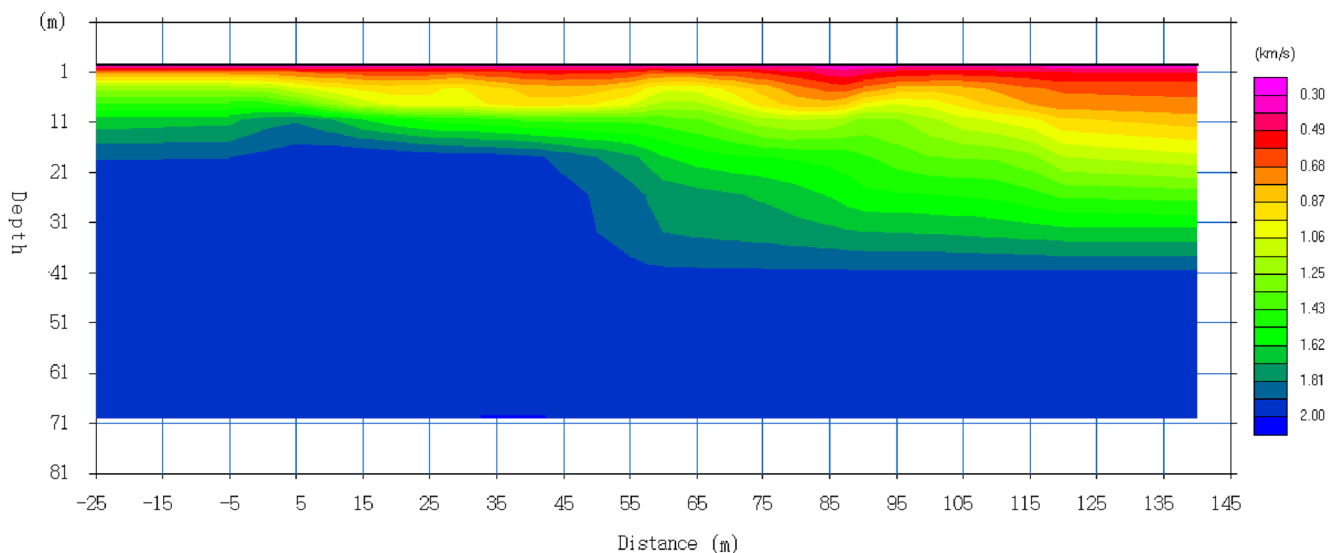


Fig. 5 Geoseismic velocity model from the P-wave seismic refraction profile in the study area

Table 6 *N* value classes (modified after Bowels 1984)

Cohesive soil		Cohesionless soil	
<i>N</i> value	Description	<i>N</i> value	Description
< 4	Very soft	0–10	Loose
4–6	Soft	11–30	Medium
7–15	Medium	31–50	Dense
16–25	Stiff	> 50	Very dense
> 25	Hard		

defines the ratio of shear stress to shear strain. In the study area of Jizan City, shear modulus values ranged from 1.23 to 30.253×10^8 dyn/cm² (Fig. 9). Bulk modulus reflects a material’s ability to tolerate volume changes in all directions when subjected to compression. The bulk modulus (*K*) of Jizan City varied between 2.0 and 50.372×10^8 dyn/cm² (Fig. 10).

Soil competence scale

Soil competence parameters including *N* value, density gradient (*D_i*), material index (*M_i*), concentration index (*C_i*), stress ratio (*S_i*), and ultimate bearing capacity (*Q_{ult}*) have been estimated. The resistance to liquefaction of soil has been evaluated in terms of *N* value using the Stumpel et al. (1984) formula

(Table 3). The *N* value is commonly used in both cohesive and non-cohesive deposits where materials with low competence show a low *N* value and vice versa. For the Jizan studied area, there is a distinct heterogeneity of the *N* value with the depth as it increases at a certain depth under *V_S* sites while it decreases at the same depth below other sites, although it increases with the depth in general (Fig. 11).

The density gradient represents an increase in bulk density under load or tectonic stresses Cordier (1985). This means that the density gradient represents the consolidation state. In the Jizan area, the topsoil profile had a density gradient ranging from 1.15 to 1.56 gm/cm³ (Fig. 12), indicating a broad variation in compaction degree. The stress ratio affects the fluid pressure. Therefore,

Fig. 6 Shear wave velocity (*V_S*) profiles distributed within the Jizan area

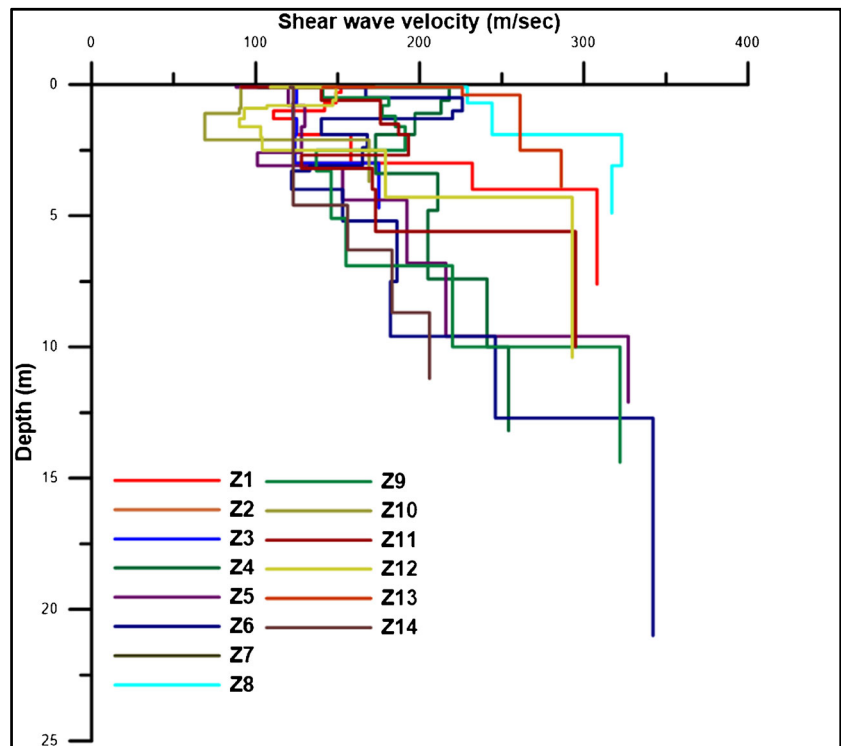
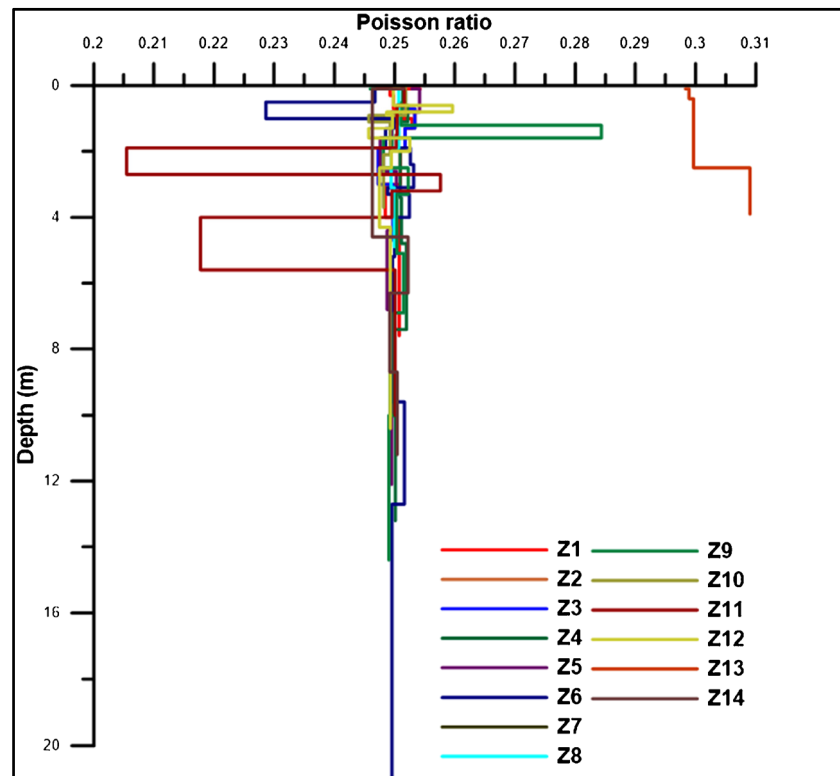


Fig. 7 Poisson's ratio computed in the studied area



formations with high fluid pressure have low velocity and low differential pressure. Moreover, the topsoil profiles of the Jizan study area is subject to vertical and horizontal stresses due to pore-filling fluids. Depending on the Cordier hypothesis (1985), these formations are sub-compacted or overpressured zones often occurring in recent unconsolidated sedimentary sequences. Soils are graded as soft, moderately compacted, and compacted according to stress ratio. Higher stress ratio values display less competent/compacted soil and vice versa. The stress ratio in the studied area ranged between 0.33 and 0.56 (Fig. 13), suggesting a significant heterogeneity throughout the Jizan area.

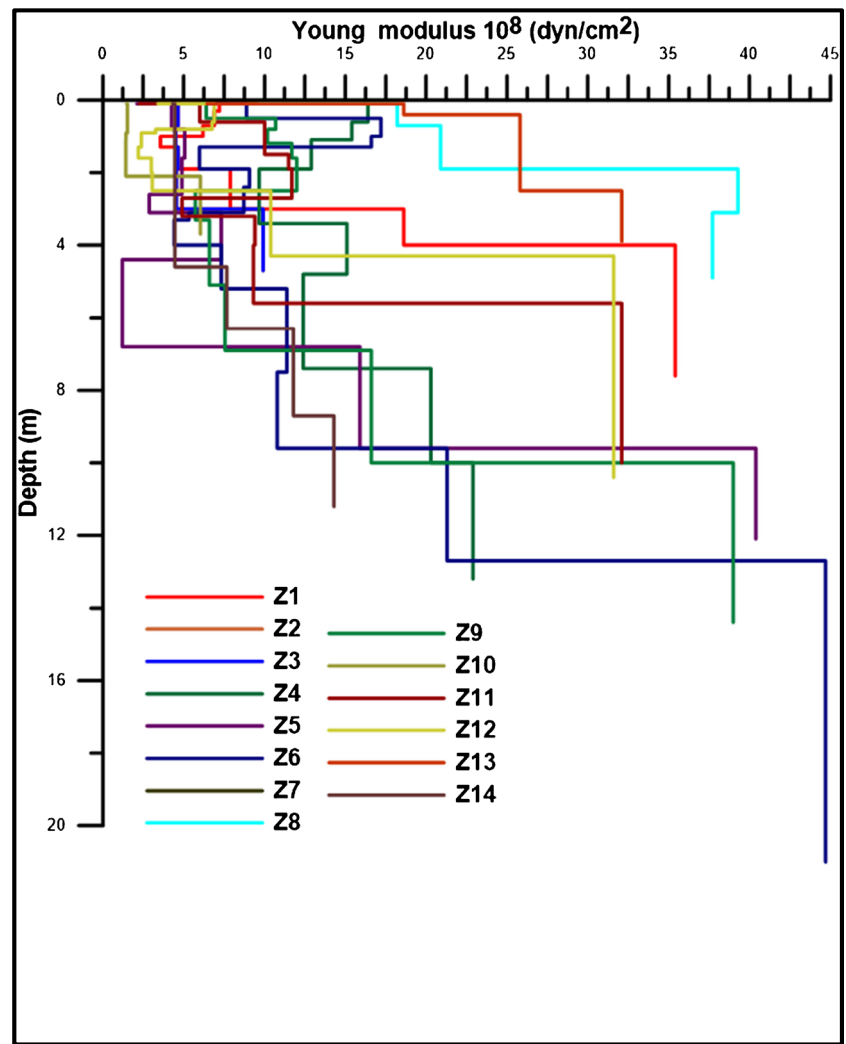
The material index (M_i) represents the competence degree of a material. It depends on both the mineralogical composition and physical environment affecting the soil or rocks. In general, the values of M_i vary from + 1 to - 1. In the study area, M_i values ranged from - 0.25 to + 0.18 (Fig. 14), suggesting materials with different competencies. The concentration index (C_i) defines the degree of concentration or compaction of a material. The degree of soil compaction, which corresponds to a degree of competence, is a vital parameter for both foundation and civil engineering projects. Moreover, C_i depends on changes in soil elastic constants and pressure with depth. The C_i values varied from 4.59 to 5.61 across the study area of Jizan (Fig. 15). This indicated a gradual vertical variation from soft soil to competent

soil. In this study, the topsoil profile of the Jizan area showed Q_{ult} values between 0.04 and 1.5 kg/cm² (Fig. 16), indicating soft to moderately competent materials.

Discussion and conclusions

Based on the 1D velocity models of 14 MASW profiles, it was noticed that within a depth of less than 10 m, the velocity values changed rapidly in a very low velocity range (less than 200 m/s). This indicated a rapid change in soil type and quality, and its dynamic and geological properties. This change continued as depth increased to 15 m, but to a lesser extent. This reflected an improvement in soil quality with depth or the emergence of another type of soil. When moving horizontally in the velocity range of 200–300 m/s, changes in the velocity values were also found, but not as much as the first velocity range (less than 200 m/s). This approves the existence of horizontal changes that were consistent with the vertical changes in velocity values till 15 m depth. Moving more horizontally in the direction of velocity increase (exactly in the range of 300–400 m/s), rapid changes appear again, but within a specific depth between 12 and 20 m. This feature indicates that probably at this depth the material content and dynamic properties changed.

Fig. 8 Young modulus estimated through the Jizan area

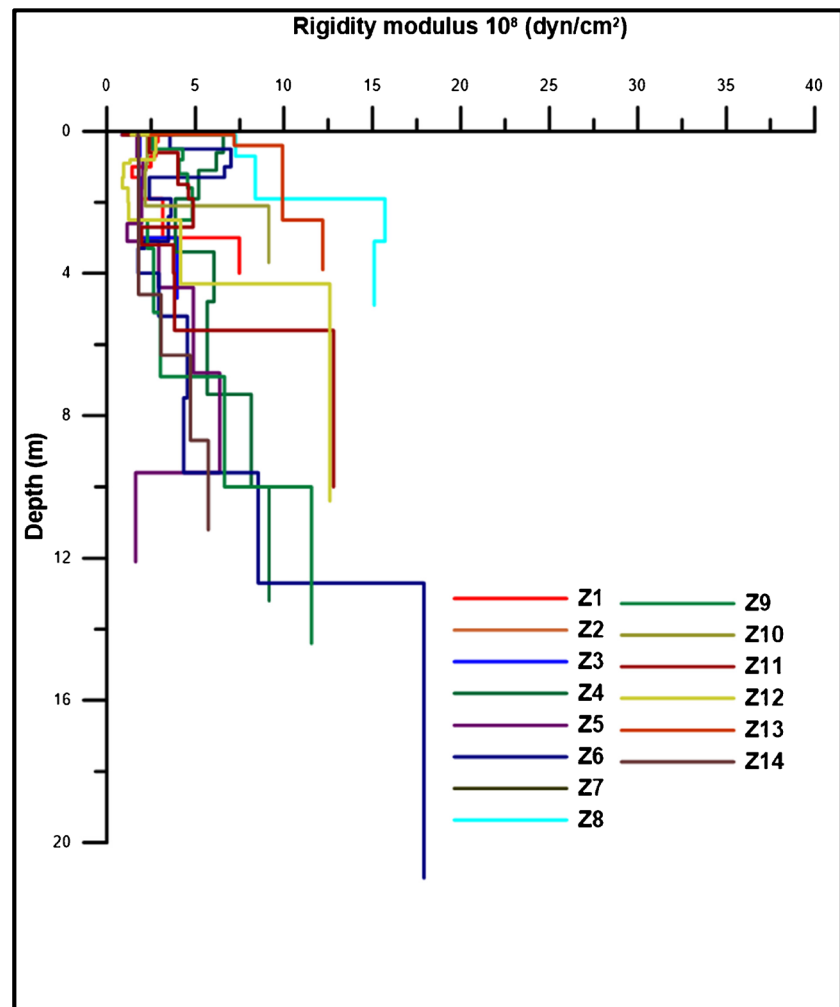


Based on dynamic constants and geotechnical properties, it was demonstrated that there are rapid and unexpected changes in horizontal and vertical lithology and density throughout the study area. Vertical changes were clarified by drawing vertical sections of these parameters at each site for both seismic refraction and MASW profiling. At these sites, soil profiles were categorized into two layers based on changes in velocity, especially shear waves (V_S), and recommendations from the Uniform Building Code (UBC). The 1st layer has variable thicknesses, ranging from 0 to 4 m depth (at site z_1), 8.4 m (z_2 and z_3), 4.8 m (z_4), 9.6 m (z_5), 7.5 m (z_6), 8 m (z_7), 0.7 m (z_8), 1.6 m (z_9), 10.2 m (z_{10}), 1.9 m (z_{11}), 10.4 m (z_{12}), 0.4 m (z_{13}), and 11.2 m (z_{14}). The average P-wave velocity (V_P) was 180–319 m/s and V_S was 99–180 m/s. This layer consisted of loose to medium cohesionless soils, or mainly soft to hard cohesive soils, depending on the subsoil class based on UBC and V_S30 values (S^{eco} EPinto 2002; Sabetta and

Bommer 2002). The V_P of the second layer was in the range of 325–1000 m/s, but the range of V_S was 180–360 m/s. This layer is constituted by dense to medium-dense sand, gravel, or stiff clay. This layer extended to the depths of 12 m (z_1), 16.7 m (z_4), 12.1 m (z_5), 31.5 m (z_6), 6.4 m (z_8), 23.2 m (z_9), 10 m (z_{11}), 20.6 m (z_{12}), 8.8 m (z_{13}), and 14.2 m (z_{14}). These results clearly showed the lateral and vertical variations of seismic velocity affecting the dynamic and geotechnical characteristics of soil profiles across the Jizan study area.

The dynamic features were calculated for two upper layers (Figs. 17 and 18). The rigidity modulus varied from 0.12 to 0.48×10^9 dyn/cm² for the first layer. The rigidity modulus contour map indicates the low rigidity zone covering the central part including the z_5 , z_{14} , z_9 , z_3 , z_2 , z_{10} , z_1 , and z_{12} sites, while these values increased eastward and westward. The rigidity modulus ranged from 0.4 to 1.35×10^9 dyn/cm² for the second layer. The rigidity modulus contour map of the second layer showed increasing values westward. The bulk modulus

Fig. 9 Shear modulus calculated in the investigated area



of the first layer ranged from 0.2 to 0.78×10^9 , indicating a zone of low bulk modulus that passes through the central zone of the map. Instead, the bulk modulus of the second layer diverged from 0.8 to 3.2×10^9 dyn/cm^2 and increased westward. Also, the Young's modulus of the first layer ranged from 0.3 to 1.2×10^9 , providing a low-value zone in the central part. However, these values increase eastward and westward. In comparison, the Young's modulus of the second layer ranged from 1.0 to 3.3×10^9 , showing an increase westward. Similarly, the Poisson's ratio extended from 0.22 to 0.3 in the first layer and 0.21 to 0.34 in the second layer. The contour maps of the upper two layers present an increasing westward, suggesting that the western region has fairly competent materials. However, the eastern part showed competent materials. Lastly, the Q_{ult} extends from 0.04 to 0.24 kg/cm^2 in the first layer and 0.2 to 1.05 kg/cm^2 in the second layer. According to Table 5, these results indicate fairly competent materials for the upper two layers.

The soil competence properties were contoured (Figs. 19 and 20) for both the first and second layers to facilitate the

comparison process. The density gradient (M_i) ranged from 1.13 to 1.33 in the 1st layer showing the low-density zone at z_5 , z_3 , z_2 , z_{10} , and z_{12} , and the density increased eastward and westward. This index varied from 1.31 to 1.51 for the second layer and increased eastward. Also, the concentration index (C_i) varied from 4.35 to 5.6 for the first layer and from 4.0 to 5.8 for the second layer. The contour maps for C_i indicated these values increased eastward for both layers. According to Table 6, both first and second layers contain a broad variety of materials ranging from soft to fairly competent and competent. Similarly, the material index ranged from -0.25 to $+0.14$ for the first layers and -0.34 to $+0.18$ for the second layer. The M_i contour maps indicated an eastward increase in index values at sites z_7 , z_8 , and z_{13} where the M_i values were low. According to Table 6, the M_i values suggested a wide range of incompetent, fairly competent to competent materials. Finally, the values of stress ratio (S_i) ranged from 0.28 to 0.43 for the first layer, indicating fairly competent to competent materials. Moreover, the S_i values varied from 0.27 to 0.51 in the second layer, suggesting soft to fairly competent and competent

Fig. 10 Bulk modulus in the studied area

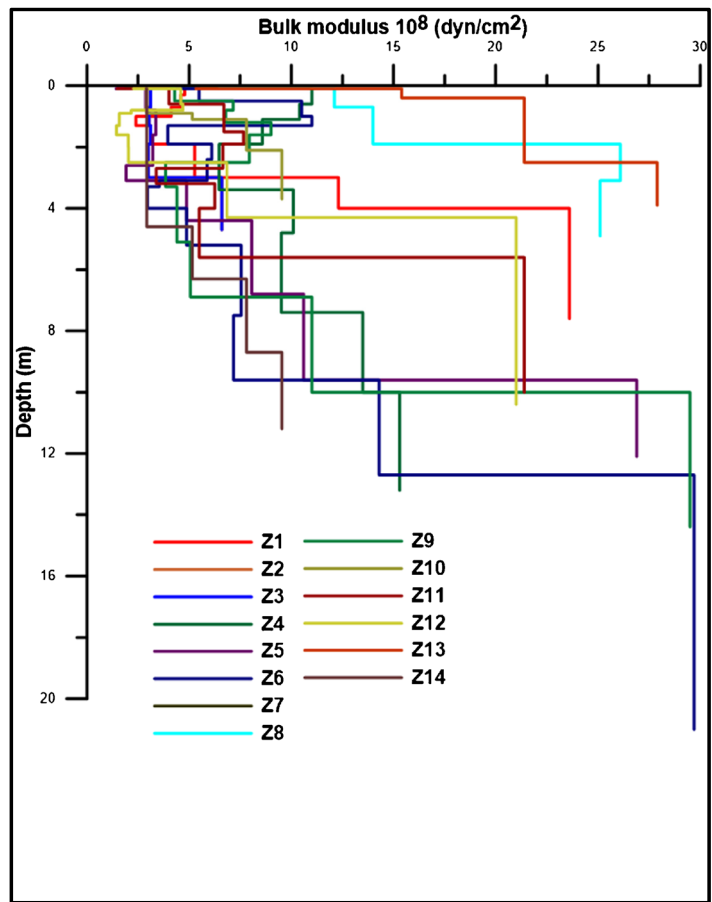


Fig. 11 N-value distribution in the investigated area

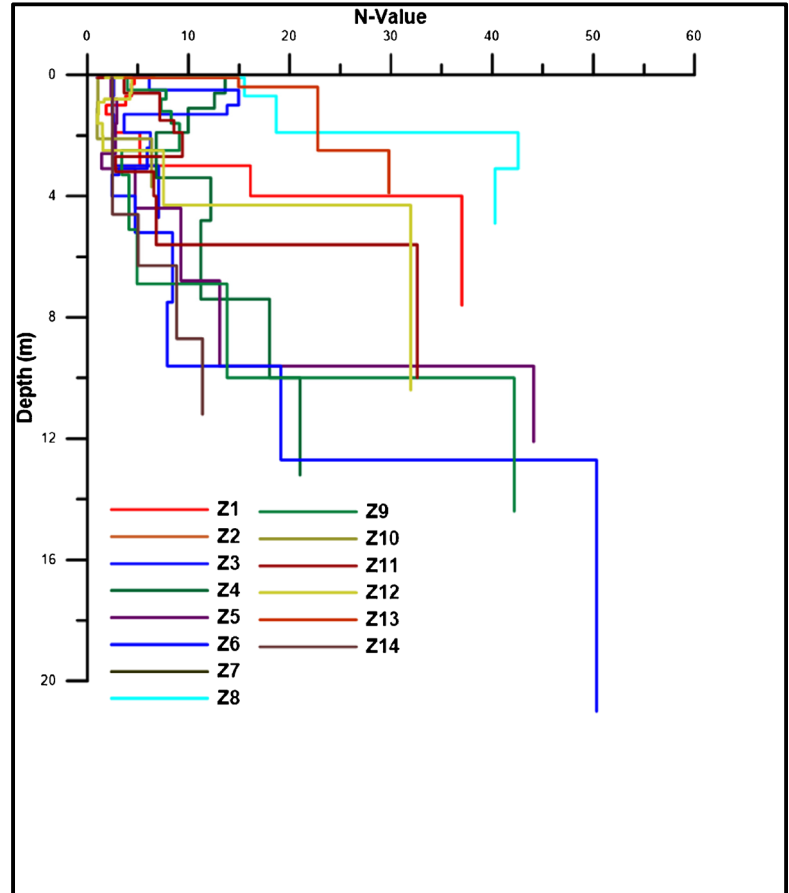


Fig. 12 Density gradient as deduced in the studied area

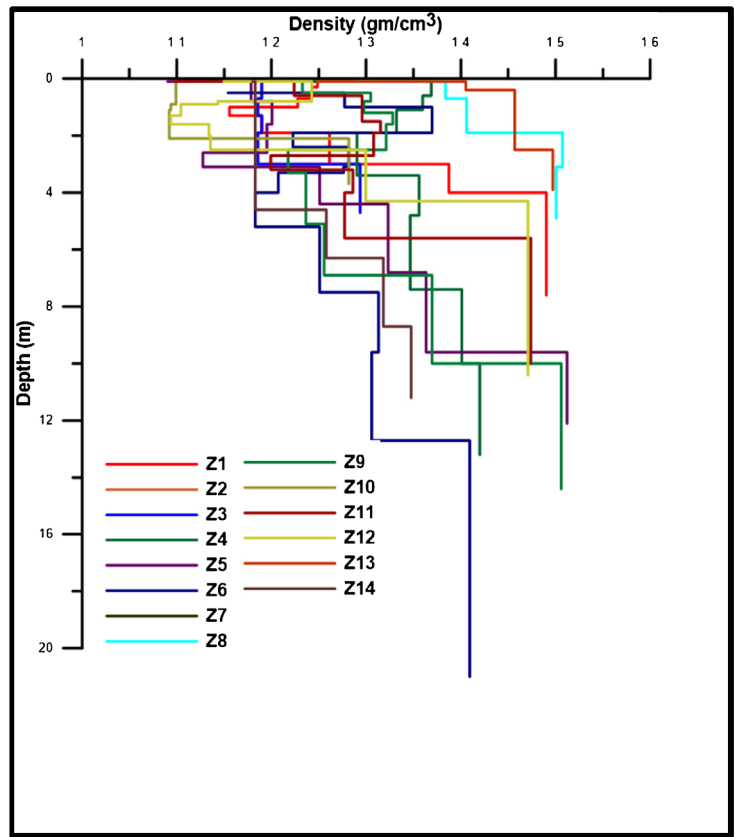


Fig. 13 Stress ratio estimated for the Jizan area

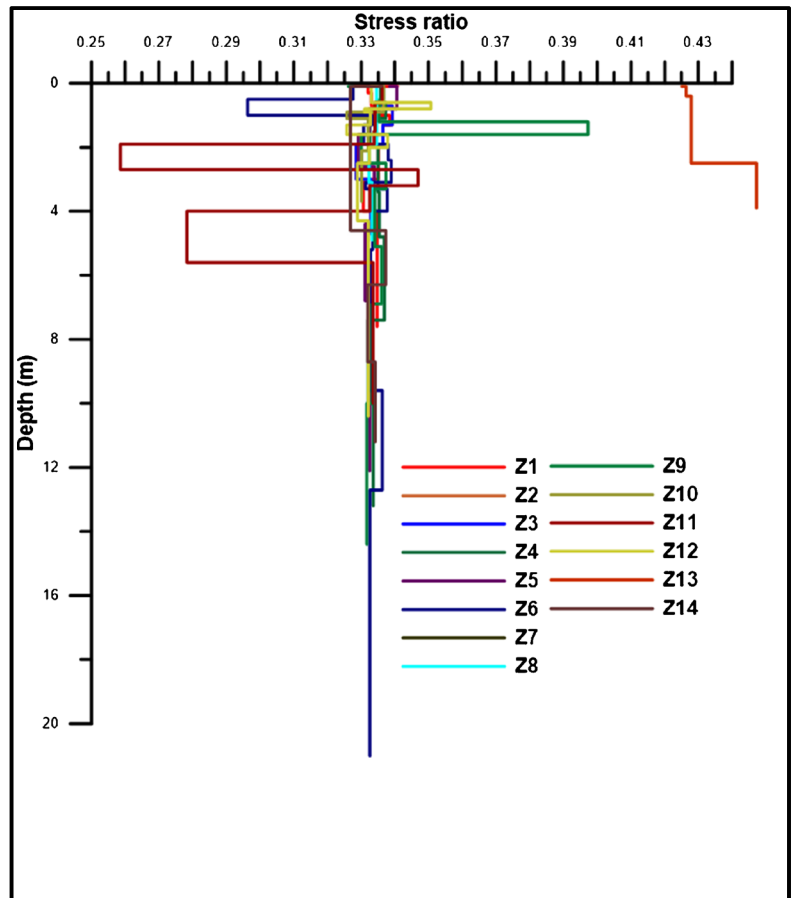


Fig. 14 Material index as distributed in the investigated area

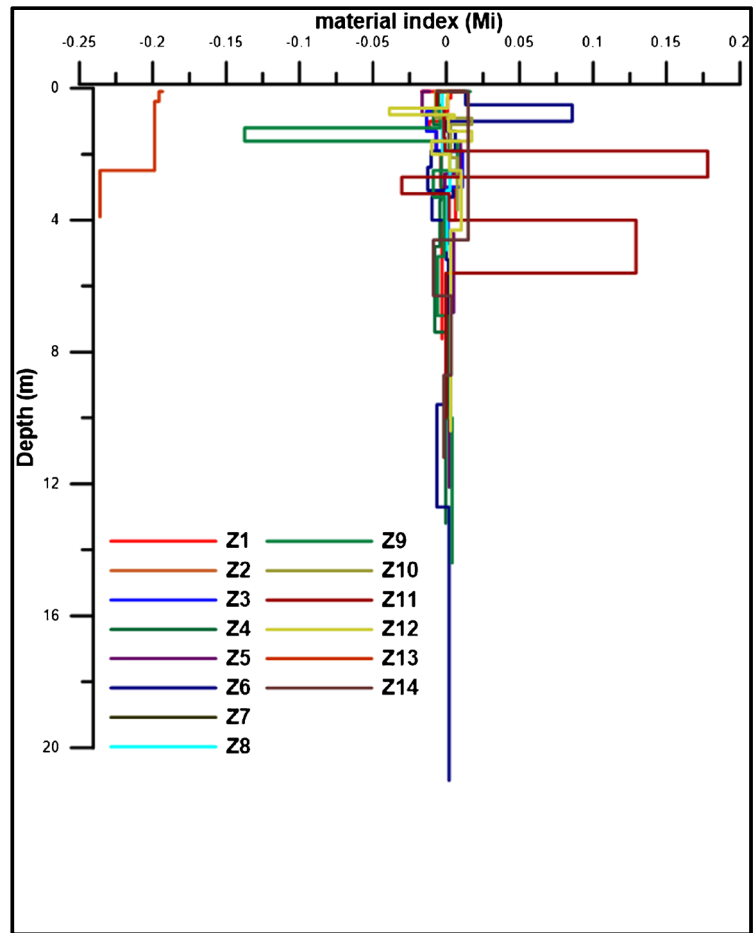


Fig. 15 Concentration index as distributed in the studied area

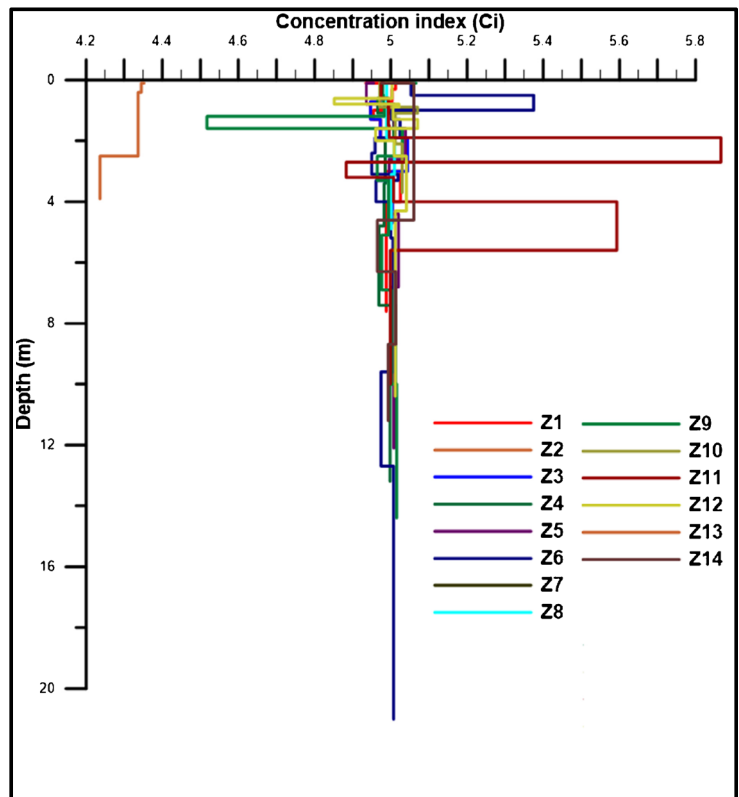


Fig. 16 Ultimate bearing capacity values estimated in the area of study

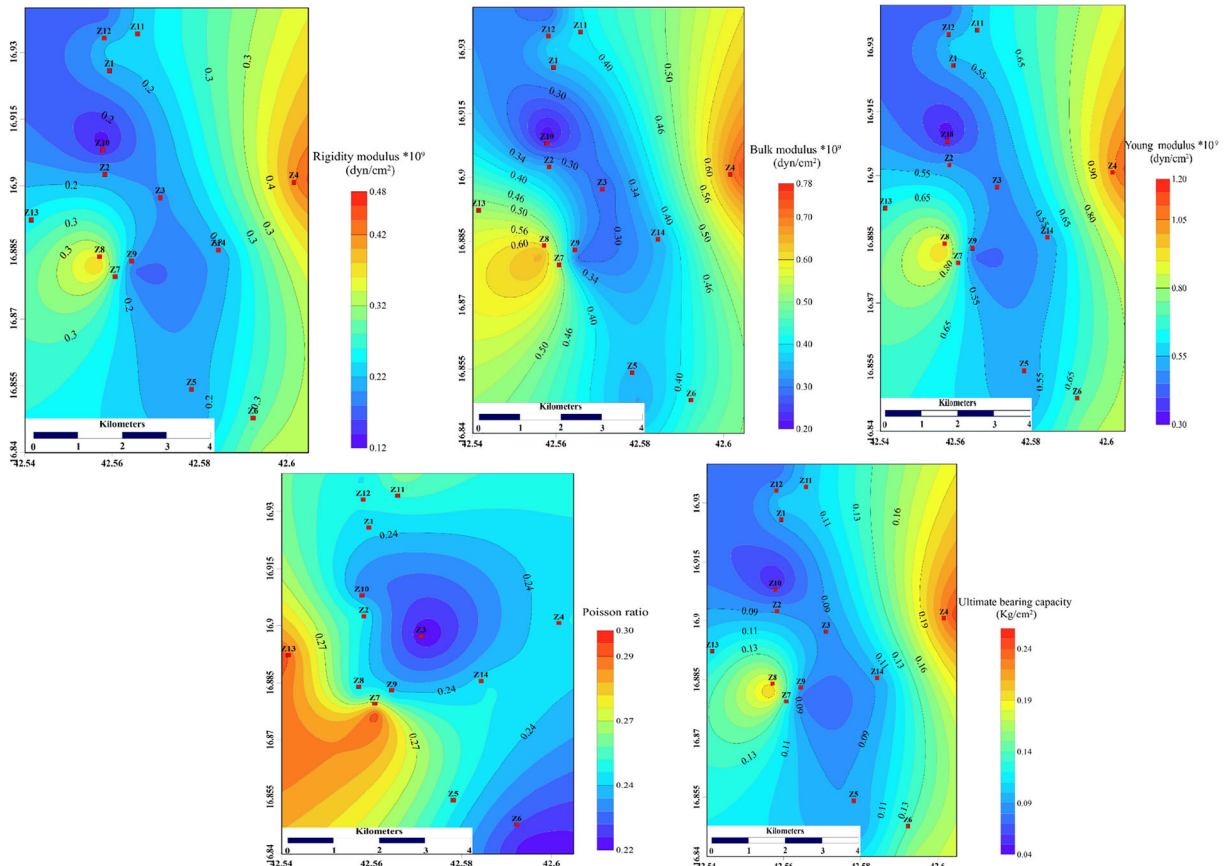
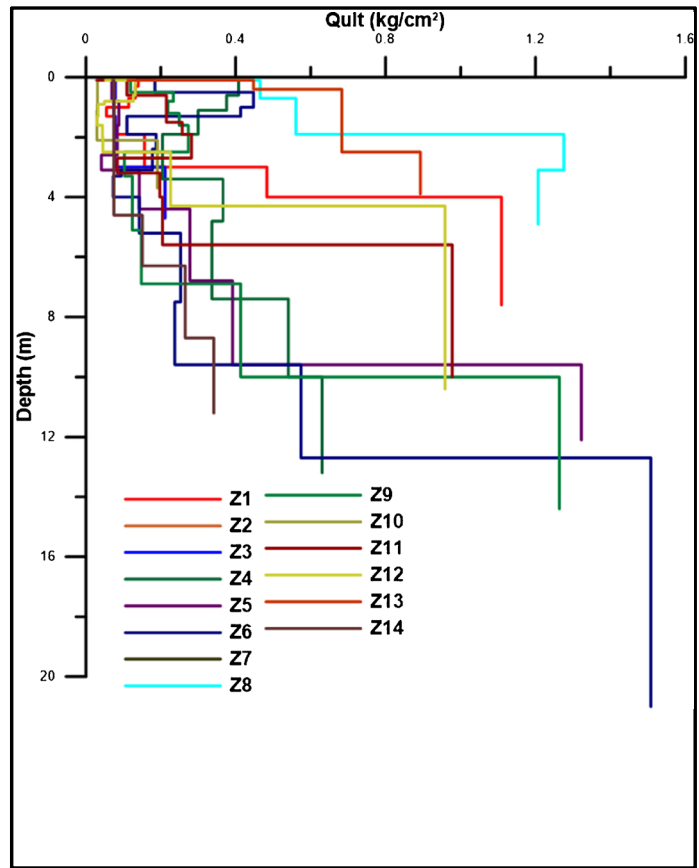


Fig. 17 Distribution of dynamic parameters as deduced for the first layer

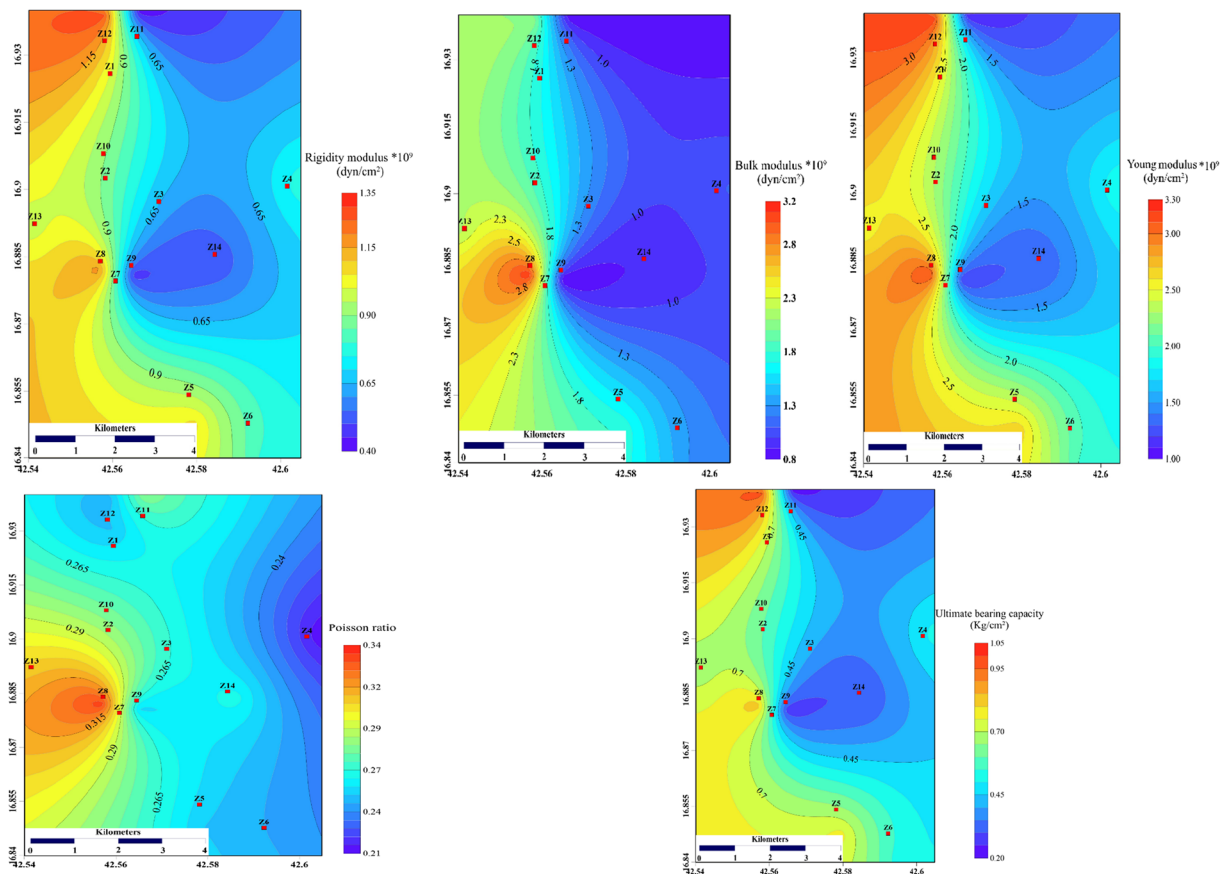


Fig. 18 Distribution of dynamic parameters as deduced for the second layer

materials. The S_i values increased westward (including Z_7 , Z_8 , Z_{13} , Z_2 , and Z_{10}), suggesting soft to fairly competent materials, while the materials in the eastern part were competent.

To assess the engineering problems encountered in Jizan City, the dynamic characteristics and geotechnical parameters were evaluated. It was revealed that the topsoil profile can be classified into two layers based on noticeable changes in shear wave velocity. The thickness of the first layer diverged from 0 to 11.2 m, overlying the second layer with varying thickness reaching a depth of 31.5 m. The geotechnical parameters of the topsoil profile revealed soft to fairly competent soil in the first layer and moderately competent soil in the second layer. Moreover, the ultimate bearing capacity (Q_{ult}) indicated that a zone of weak soil covers the central zone and extends NW-SE. This zone cannot be classified as a foundation layer for high-rise buildings and heavy equipment, especially when the soil is highly water-saturated. Thus, sand liquefaction, foundation failure, land subsidence, and damage to buildings are highly expected in Jizan City. In conclusion, extensive variations in topsoil profiles in terms of lithology and dynamic and geotechnical properties can cause engineering problems in the new or renovated buildings, roads, and infrastructure in Jizan. The engineering treatment of weak soil across the Jizan study area is highly recommended before constructing new buildings, roads, and infrastructure.

Acknowledgments This research was funded by the National Plan for Science, Technology and Innovation (MAARIFAH), King Abdulaziz City for Science and Technology, Kingdom of Saudi Arabia, Award Number (2-17-01-001-0014).

References

- Abd El Rahman M (1989) Evaluation of the kinetic moduli of the surface materials and application to engineering geologic maps at Ma'Barrisabah area (Dhamar Province), Western Yemen. *Egypt J Geol* 33:229–250
- Abd El Rahman M (1991) Rock material competence assessed by seismic measurements with emphasis on soil competence scale and applications in some urban areas in Yemen. *E.G.S. Proc. of the 9th Ann. Meet.*; pp.206–228
- Abd El Rahman M, Abd El Latif T (1990) Geophysical interpretations for shallow engineering site investigations at the area north of Sana'a, Yemen Arab Republic. *Merc.* 4:41–51
- Abd El Rahman M, Setto I, El Werr A (1991) Seismic refraction interpretation for shallow engineering site investigations at the distinctive district 6th of October City. *E.G.S. Proc. of the 9th Ann. Meet.*; pp.229–242
- Abdelrahman K, Al-Amri AM, Al-Otaibi N, Fnais M (2020) Geotechnical assessment for the ground conditions in Makah Al-Mukarramah city, Saudi Arabia. *J King Saud Univ Sci* 32:2112–2121
- Abu-Hajar IH (1991) Ground conditions in Jeddah and its influence on selection and design of foundation. *JKAU, Earh Sci* 4:45–66
- Adams LH (1951) Elastic properties of materials of the earth's crust. *Internal Construction of the Earth* (edited by Gutenberg). Dover publications, Inc, New York

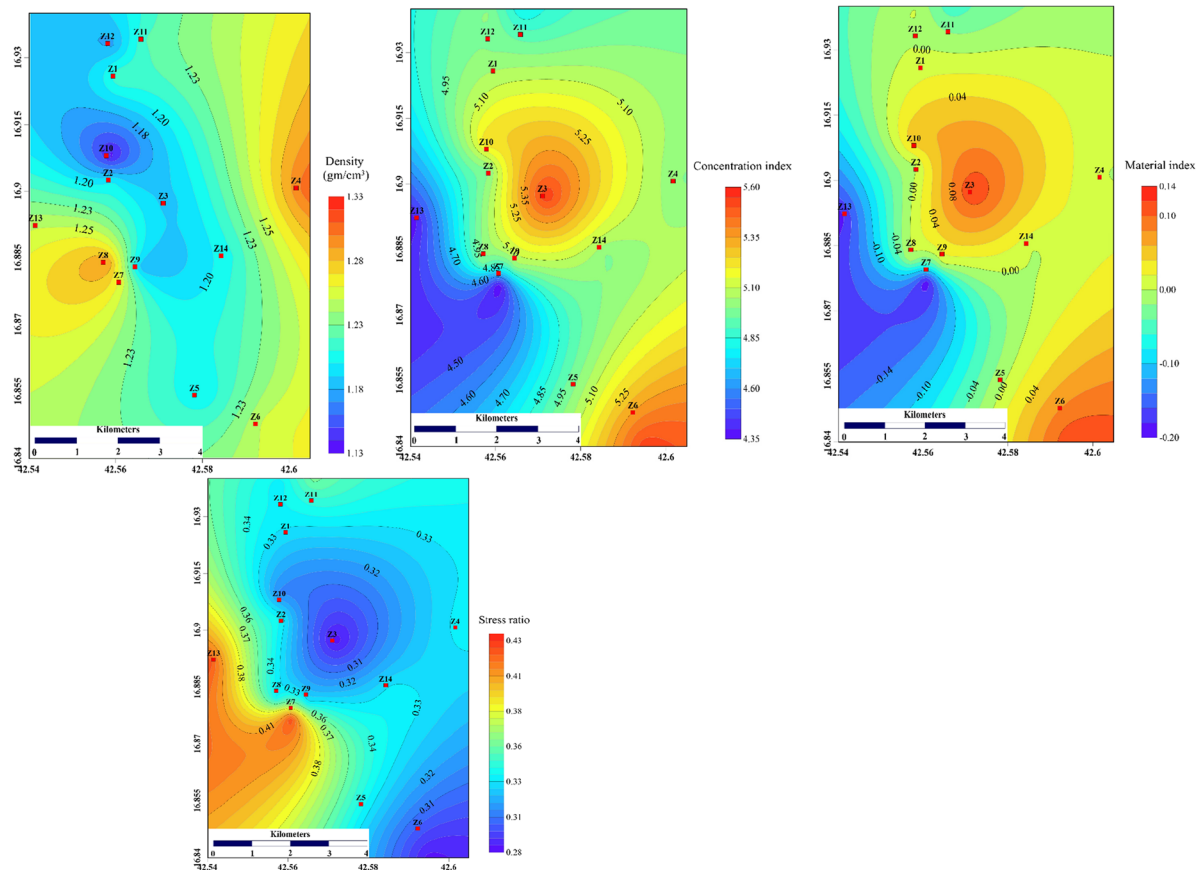


Fig. 19 Geotechnical parameters as defined for the first layer

- Aggour MS, Radding WR (2001) Maryland State Highway Administration Rep. No. *MD02-007B48*
- Al-Amoudi OSB (1992) Studies on soil-foundation interaction in the Sabkha environment of eastern province of Saudi Arabia. [PhD Dissertation]. Dhahran, Saudi Arabia: Department of civil engineering, King Fahd University of Petroleum and Minerals
- Al-Amoudi OSB, Abduljawwad SN, El-Naggar ZR, Rasheeduzzafar (1992) Response of sabkha to laboratory tests: a case study. *Eng Geol* 33:111–125
- Al-Farraj AS (2008) The mineralogy of clay fractions in the soils of the southern region of Jizan. *J Agron* 7:115–126
- Al-hadad M, Al-Refeai T, Al-Amri A (2001) Geotechnical investigation for earthquake resistant design in the Kingdom- phase 1- Western Coast. Report No. AR-14-77 submitted to the King Abdulaziz City for science and technology (KACST)
- Alhumimidi MS (2020) Geotechnical assessment of near-surface sediments and their hazardous impact: case study of Jizan city, south-western Saudi Arabia. *J King Saud Univ Sci* 32:2195–2201
- Amin A (2004) Comparative study of the geotechnical properties of the coastal Sabkhas of Saudi Arabia and their hazardous effects. *Bull Eng Geol Environ* 63:309–314. <https://doi.org/10.1007/s10064-004-0254-5>
- Anbazhagan P, Sitharam TG (2006) Evaluation of dynamic properties and ground profiles using MASW: correlation between vs and N60. 13th symposium on earthquake engineering. Roorkee: Indian Institute of Technology, Dec. 18-20, Paper No. 008
- Anderson N, Chen G, Kocui S (2003) Vertical shear-wave velocity profiles generated from spectral analysis of surface waves: field examples: Missouri Department of Transportation, Development and Technology Report, RDT; pp.03–006
- Arifuzzaman M, Habib MA, Al-Turki MK, Khan MI, Ali MM (2016) Improvement and characterization of sabkha soil of Saudi Arabia: a review. *J Teknol (Sciences & Engineering)* 78:6 78:1–11
- Birch F (1966) Handbook of physical constants. Geol. Soc. Amer. Men, v.97, p. 613
- Blank HR, Johnson PR, Gettings ME, Simmons GC (1986) Explanatory notes to the geological map of the Jizan Quadrangle, Sheet 16F, Kingdom of Saudi Arabia. Ministry of Petroleum and Mineral Resources, Jeddah
- Bowels JE (1984) Physical and geotechnical properties of soils. Mc Grew-Hill, London
- Bowles JE (1997) Foundation analysis and design fifth edition, 20 (3)
- Burland J (2007) Terzhagi: back to the future. *Bull Eng Geol Environ* 66: 29–33
- Cordier GE (1985) Velocity and refraction seismology. Reidel, Dordrecht
- Dhowian AW, Erol AO (1993) Ground conditions and associated structural problems in Jizan and Tabuk Region. Final Report of the Contract No. AR-8-106, Research Grant Supported by King Abdulaziz City for Science and Technology (KACST)
- Dhowian AW, Erol AO, Sultan S (1987) Settlement predictions in complex sabkha soil profiles. *Bull Int Assoc Eng Geol Paris* 36:11–21
- EPinto SPS (2002) Eurocode 8-design provisions for geotechnical structures. Special lecture, 3rd Croatian Soil Mechanics and Geotechnical Engineering Conference, 2002 Harvard
- Erol O, Dhowian AW (1988) June 1–5. Proc. Second International Conference on Case Histories in Geotechnical Engineering No. 2. Plain: Foundation Failures Associated with Salt Rock and Surrounding Coastal. St. Louis: Paper, p. 39
- Gardner GHF, Gardner LW, Gregory AR (1974) Formation velocity and density – the diagnostic basics for stratigraphic traps. *Geophysics* 39:770–780

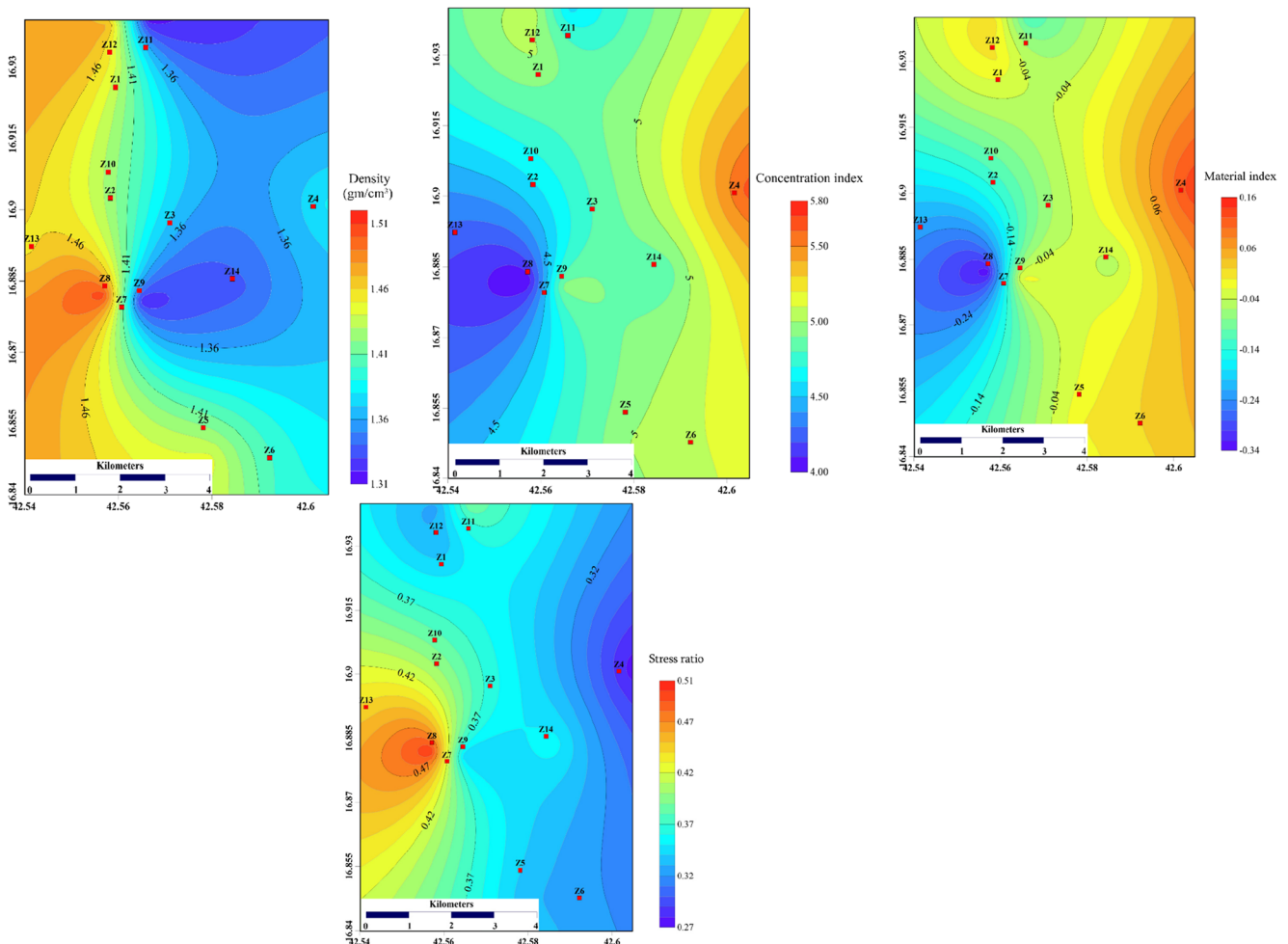


Fig. 20 Geotechnical parameters as defined for the second layer

- Ghazali FM, Fatani MN, Khan AM (1986) Geotechnical properties of sabkha soils of Jeddah and Jizan, Saudi Arabia. Proc. Second Saudi Engineers Conference, Dhahran, Saudi Arabia; p. 287-3CY7
- Hodgson IF, Caronna S, Taleb MG (1989) Geotechnical aspects of a development project for the coastal town of Jizan, Second Symposium on Geotechnical Problems in Saudi Arabia. Saudi Arabia: University of Riyadh
- Imai S (1975) An investigation to geophysical prospecting for civil purposes. OYO Corporation, Tokyo
- Kramer SL (1996) Geotechnical earthquake engineering. Upper Saddle River, Prentice Hall, p 07458
- Kulhawy FH, Mayne PW (1990) Manual on estimating soil properties for foundation. Design
- Mahfouz AH (2016) Geotechnical study of soil foundation and design of PCC piles to improve its bearing capacity, a case study: ramps of Dawar El-Tawheed Bridge in Jizan City –kSA. Int J Forest Soil Erosion (IJFSE) 6:140–157
- Matsah MI, Hossain D (1993) Ground conditions in Al-Madinah Al-Munawarah, Saudi Arabia. J KAU 6:47–77
- Miller RD, Xia J, Park CB, Ivanov JM (1999) Multichannel analysis of surface waves to map bedrock. Lead Edge 18:1392–1396
- Park CB, Miller RD, Xia J (1999) Multichannel analysis of surface waves. Geophysics 64:800–808
- Ravi S (2017) Geotechnical investigations in difficult ground conditions – Indian experiences. Sixth Madhav Lecture, JNTU. Hyderabad: October
- Roy S, Bhalla SK (2017) Role of geotechnical properties of soil on civil engineering structures. Resour Environ 7:103–109. <https://doi.org/10.5923/j.re.20170704.03>
- Sabetta F, Bommer J (2002) Modification of the spectral shapes and subsoil conditions in Eurocode. 12th European Conference on Earthquake Engineering, paper ref 8, p. 518
- Shaaban F, Ismail A, Massoud U (2013) Geotechnical assessment of ground conditions around a tilted building in Cairo–Egypt using geophysical approaches. J Assoc Arab Univ Basic Appl Sci 13: 63–72
- Sjogren B, Ofsthus A, Sandberg J (1979) Seismic classification of rock mass qualities. Geophys Prospect 27:409–442
- Stipho AS (1984) Soil conditions and foundation problems in the desert region of the Middle East. <https://scholarsmine.mst.edu/icchge/licchge/licchge-theme1/53>. 1st international conference on case histories in geotechnical engineering, 53
- Stumpel H, Kahler S, Meissner R, Milkereit B (1984) The use of seismic shear waves and compressional waves for lithological problems of shallow sediments. Geophys Prospect 32:662–675
- Tatham RH (1982) Vp/Vs and lithology. Geophysics 47:336–344. <https://doi.org/10.1190/1.1441339>
- Terzaghi K (1940) Purdue Conference on Soil Mechanics and its Applications 151
- Terzaghi K, Peck RB (1948) Soil mechanics in engineering practice
- Xia J, Miller RD, Park CB (1999) Estimation of near-surface shear-wave velocity by inversion of Rayleigh waves. Geophysics 64:691–700

